

PAPER

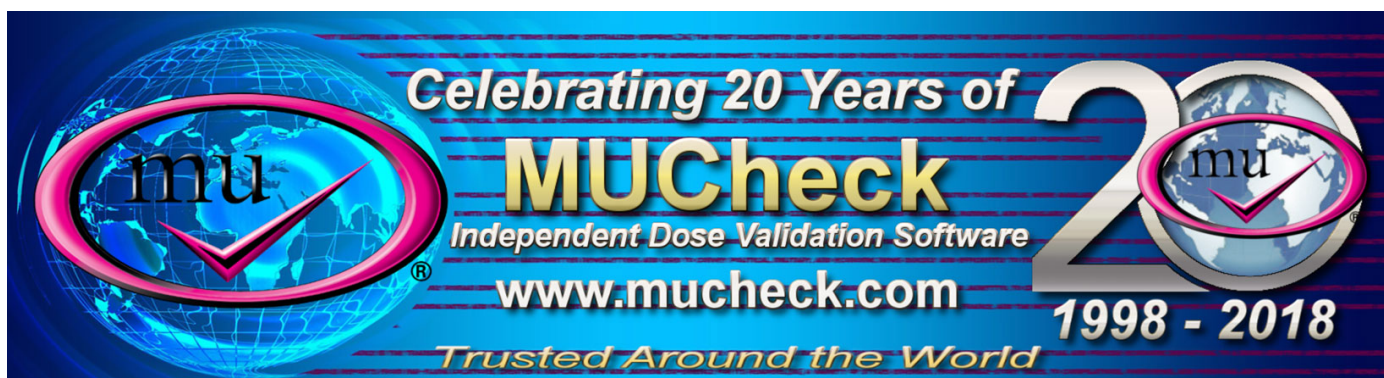
Streamlined open-source gel dosimetry analysis in 3D slicer

To cite this article: K M Alexander *et al* 2018 *Biomed. Phys. Eng. Express* **4** 045041

View the [article online](#) for updates and enhancements.

Related content

- [Implementation of an efficient workflow process for gel dosimetry using 3D Slicer](#)
K M Alexander, C Pinter, J Andrea et al.
- [A fast dual wavelength laser beam fluid-less optical CT scanner for radiotherapy 3D gel dosimetry II: dosimetric performance](#)
Daniel Ramm
- [Three-dimensional small field dosimetry with radiochromic gels](#)
Steven Babic, Andrea McNiven, Jerry Battista et al.



Biomedical Physics & Engineering Express



PAPER

Streamlined open-source gel dosimetry analysis in 3D slicer

K M Alexander¹ , C Pinter² , G Fichtinger², T Olding^{1,3,4} and L J Schreiner^{1,3,4}¹ Department of Physics, Queen's University, Kingston, ON, K7L 3N6, Canada² School of Computing, Queen's University, Kingston, ON, K7L 3N6, Canada³ Cancer Centre of Southeastern Ontario at Kingston General Hospital, 25 King Street West, Kingston, ON, K7L 5P9, Canada⁴ Department of Oncology, Queen's University, Kingston, ON, K7L 3N6, CanadaE-mail: k.alexander@queensu.ca**Keywords:** radiation therapy, 3d dosimetry, gel dosimetry

RECEIVED

10 May 2018

REVISED

14 June 2018

ACCEPTED FOR PUBLICATION

3 July 2018

PUBLISHED

19 July 2018

Abstract

Three dimensional dosimetry is being used in an increasingly wide variety of clinical applications as more gel and radiochromic plastic dosimeters become available. However, accessible 3D dosimetry analysis tools have not kept pace. 3D dosimetry data analysis is time consuming and laborious, creating a barrier to entry for busy clinical environments. To help in the adoption of 3D dosimetry, we have produced a streamlined, open-source dosimetry analysis system by developing a custom extension in 3D Slicer, called the Gel Dosimetry Analysis slicelet, which enables rapid and accurate data analysis. To assist those interested in adopting 3D dosimetry in their clinic or those unfamiliar with what is involved in a 3D dosimeter experiment, we first present the workflow of a typical gel dosimetry experiment. This is followed by the results of experiments used to validate, step-wise, each component of our software. Overall, our software has made a full 3D gel dosimeter analysis roughly 20 times faster than previous analysis systems.

1. Introduction

In recent years 3D conformal radiation therapy (RT) techniques, such as intensity modulated radiation therapy (IMRT), volumetric modulated arc therapy (VMAT), and stereotactic ablative radiotherapy (SABR) have advanced dramatically. Radiation dose distributions for these treatments feature steep dose gradients, as the treatment is intended to deliver high dose to the tumour while minimizing dose to any adjacent healthy tissue. Such treatments are highly complex, making quality assurance for clinical processes, radiation treatment delivery units, and patient specific treatments an important part of ensuring that the radiation dose is delivered accurately and precisely (Low 2015, Schreiner 2015).

In the clinic, point-dose measurements and two-dimensional dosimetry techniques are commonly used to measure radiation dose (Zeidan *et al* 2006, Arjomandy *et al* 2008, Menegotti *et al* 2008, Li *et al* 2009, Devic 2011). But, these measurement techniques provide only a limited characterization of the delivered dose throughout a volume of interest. Other clinical dosimetry tools such as detector arrays provide a pseudo-3D verification of the dose delivery as a full 3D dose distribution is calculated

from coarse resolution dose measurements (Mijnheer *et al* 2010, Schreiner 2011). 3D gel dosimeters that can be read out using a high resolution 3D imaging system allow for a more complete evaluation of complex radiation dose deliveries. In Kingston, we routinely use gel dosimeters (together with other point and 2D detectors) as part of the process of commissioning new RT techniques. The tissue equivalence of, and 3D dose measurement from, gel dosimeters enable the user to replicate the treatment scenario and ensure that the treatment technique is accurate and reliable (Olding *et al* 2013, Nasr *et al* 2015, Olding *et al* 2015).

Routine clinical use of gel dosimetry has great potential. Recent developments in gel dosimetry formulations and manufacturing procedures have made producing gels in the lab more feasible (Babic *et al* 2008, Nasr *et al* 2015) and some commercial vendors (e.g., Modus Medical Devices Inc., London, ON; Presage, Skillman, NJ; RTsafe, Athens, Greece) now manufacture 3D dosimeters (radiochromic plastic and gels) that can be shipped around the world for clinical use (Adamovics and Maryanski 2006, Guo *et al* 2006, Penev and Mequanint 2015). While these have enabled better access to gel dosimeters, users need a simple, fast, and reliable way to analyze the data

obtained from the readout of an irradiated gel dosimeter, convert those data to measured doses, and compare the measurement to the planned radiation delivery.

A huge barrier impeding clinics from adopting gel dosimetry is the elaborate workflow and data analysis involved. Typical gel dosimeter analysis includes: importing data from a variety of platforms, image-based and fiducial-based image registrations (to spatially align imaging volumes from different sources), calibration (to relate a measured quantity such as optical attenuation for optical CT, or relaxation time for magnetic resonance imaging, to dose), and dose comparison between a calibrated gel measurement and a treatment planning system calculated dose distribution. Early adopters of gel dosimetry used multiple software environments to analyze their gel dosimeter data and users were forced to develop their own custom scripts/software (Murry and Baldock 2000). Gel dosimetry analysis in Kingston previously used custom scripts written in Matlab (Mathworks, Natick, MA) which were case-specific for each experiment (e.g., different gel dosimeter jar sizes, calibration procedures etc.). These scripts additionally utilized Computational Environment for Radiotherapy Research (CERR, <http://www.cerr.info>) and Microsoft Excel software to analyze our gel dosimetry data. These custom-built routines were not particularly user-friendly, not always well documented for future use, and not supported by a moderated developer community. This former method took a long time to learn, involving substantial training and hands-on experience. As well, the dosimetry process to analyze the 3D dose data from each gel dosimeter study was time consuming. The complex process also resulted in the data analysis being very user dependent, which generated questions regarding its reliability and accuracy. On a larger scale, the fact that clinics around the world used a variety of custom tools and software (which were not necessarily validated) to perform their gel dosimetry analysis, made comparison of results of 3D dosimetric studies performed between clinics even more challenging.

Streamlining and standardization of the workflow was made possible by building software tailored to the analysis process. We chose to use a software platform for our work as it helps in minimizing parallel efforts, builds on high quality tools already available, and produces a faster and more robust analysis system. 3D Slicer (<http://slicer.org>) was chosen for this work as it is an open-source and customizable computational platform that has been developed over two decades by the National Institutes of Health and developers across the world to bring image analysis, processing, and visualization tools to researchers and clinicians. The 3D Slicer environment features various registration techniques, slice viewers, advanced volume rendering, interactive segmentation, and also has a large library of downloadable extensions. To provide general

radiation therapy specific functionality and to serve as a medium between commercial treatment planning systems and research platforms, a tailored toolbox of 3D Slicer, called SlicerRT (Pinter *et al* 2012), has been developed. SlicerRT allows for loading of digital radiation therapy planning and imaging data, manipulation of structures, computation and display of dose-volume histograms, dose-volume comparisons, and dose distribution visualization. Gel dosimetry analysis was implemented in 3D Slicer by developing a custom extension with a simplified user interface, called a *slicelet*. The gel dosimetry analysis slicelet not only provides a new gel dosimetry analysis tool, but also establishes a well laid out workflow that standardizes a typical 3D dosimetry measurement. In this publication, we describe the workflow of a typical gel dosimeter experiment and show the results of experiments to validate, step-wise, each component of the gel dosimetry analysis slicelet, in a similar manner used by Kozicki *et al* (2014) to validate the commercial software that they produced to analyze polymer gel dosimeter data.

2. Methods and materials

2.1. Overview of a gel dosimeter experiment

2.1.1. Gel manufacturing and pre-irradiation optical CT scanning

In a typical gel dosimetry experiment in Kingston, one 2L batch of gel is manufactured in-house to fill two 1L cylindrical gel dosimeter jars. The first gel jar is used to measure and evaluate the dose delivered according to a specific plan (generally placed and irradiated in a phantom). The second gel jar is used as a calibration gel to calibrate the imaging readout measurement to dose for that batch of gel using a well defined standard irradiation (in our clinic we usually use an electron beam). These two volumes are labeled as the *Measured* and *Calibration* gel jars, respectively. In this approach, the conditions for the measured and calibration gels (volume, thermal history, time between irradiation and scanning etc) are kept as similar as possible. In this work, we use Fricke xyleneol orange gels as our 3D dosimeter as they can be probed using optical CT. Reference (pre-irradiation) scans are acquired for each of the two gel jars using a Vista Optical CT Scanner (Modus Medical Devices Inc., London, Ontario). Each scan takes approximately 6 min and acquires 410 projection images under amber light (590 nm) illumination as the scanner rotates the jar by 360 degrees.

2.1.2. Gel CT simulation and treatment planning

The *Measured* gel dosimeter jar is placed in a phantom (optional metal fiducials can be placed on the phantom), a CT scan is performed (figure 1(a)), and a CT simulation imaging volume is acquired (referred to as *PlanCT*). The CT images are transferred to the Eclipse treatment planning system (Varian Medical Systems,

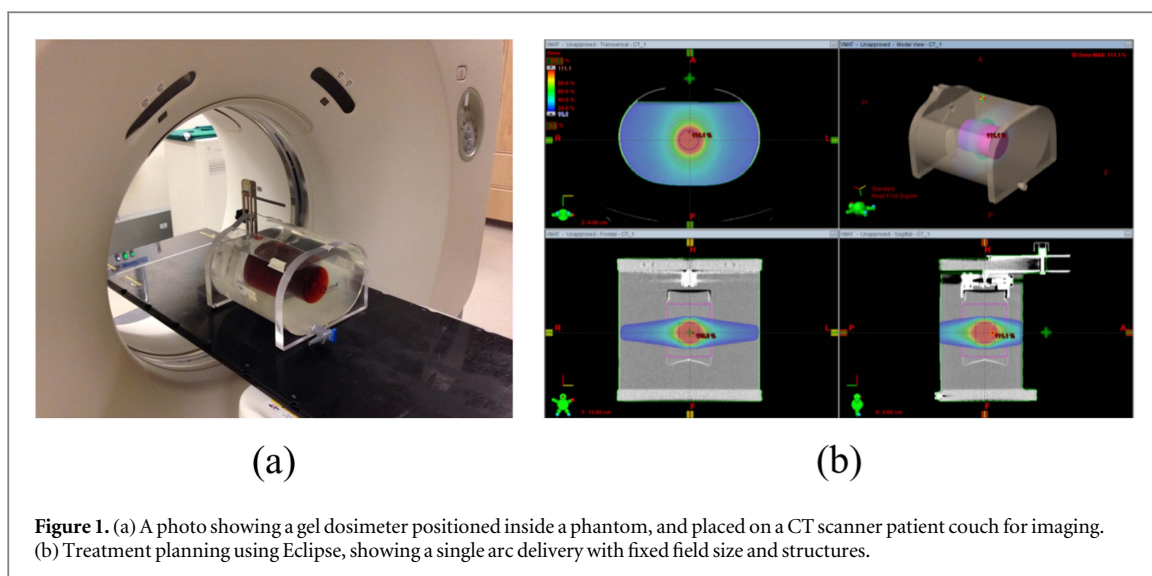


Figure 1. (a) A photo showing a gel dosimeter positioned inside a phantom, and placed on a CT scanner patient couch for imaging. (b) Treatment planning using Eclipse, showing a single arc delivery with fixed field size and structures.

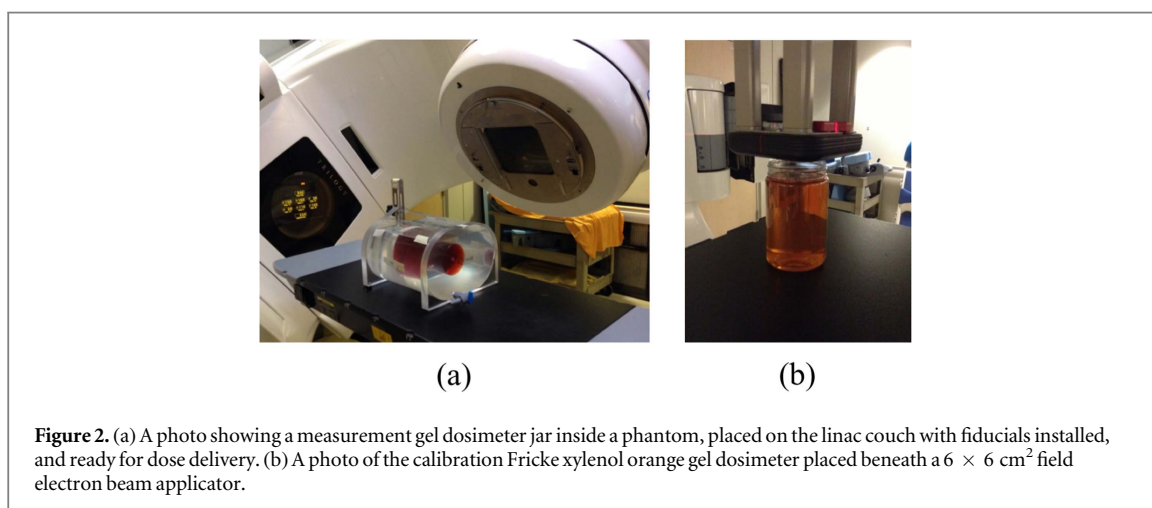


Figure 2. (a) A photo showing a measurement gel dosimeter jar inside a phantom, placed on the linac couch with fiducials installed, and ready for dose delivery. (b) A photo of the calibration Fricke xylenol orange gel dosimeter placed beneath a $6 \times 6 \text{ cm}^2$ field electron beam applicator.

Palo Alta, CA) and CT image contouring is performed (outlining the phantom body, gel jar, and any other needed structures). A radiation therapy treatment plan is then developed, and a radiation dose volume is calculated (referred to as *PlanDose*), as shown in figure 1(b).

2.1.3. Gel irradiations

A series of asymmetric pen markings are made on the measurement gel jar prior to dose delivery to act as fiducial markers to facilitate registration of the optical CT gel measurement to the calculated dose volume. These pen markings are placed away from the region of the jar that will be irradiated, as these dense optical pen markings can cause significant streaks in a reconstructed optical CT gel image, ultimately perturbing adjacent gel measurements. Radiopaque metal ball bearings (BBs) are then placed on top of each pen marking (rationale described more in section 2.2.2).

Prior to irradiation on the treatment unit, the phantom, with the *Measured* gel dosimeter jar in place, is set up in the delivery position (figure 2(a)), and the phantom setup is verified using image guidance. That

is, a cone-beam CT (CBCT) is acquired, and a 3D match with the planning CT is performed to determine if any shifts are needed to align the phantom volume with the planning CT volume. This step replicates the protocol used for each patient treatment in Kingston. Appropriate shifts are performed, if required. The CBCT x-ray imaging reveals the BBs on the gel jar and the phantom, which will help indicate the rotational orientation (here, about the longitudinal axis) of the gel at time of delivery. The phantom and gel dosimeter then undergo the planned delivery. After irradiation, the gel jar is removed from the phantom and the BBs are removed from the jar, revealing the pen fiducial markings.

Next, we irradiate the *Calibration* gel. Accurate gel dosimeter calibration is important as it defines the specific response of the gel chemistry used in a given batch, using the particular read-out system. A variety of calibration techniques can be used (Oldham *et al* 1998, Xu and Wu 2010, Olding *et al* 2011), but in our work, gel calibration is performed using the depth dose method (Alexander *et al* 2015, Ascención *et al* 2017). The calibration gel is irradiated with an

electron beam after removing the jar lid, centering the gel jar under the beam, and placing the gel at a source to surface distance (SSD) of 100 cm (figure 2(b)). A $6 \times 6 \text{ cm}^2$ field size electron beam is used as it fits nicely within the top of the jar (a 1L gel jar has a diameter of $\sim 9 \text{ cm}$). We have adopted this calibration method for our Fricke gel dosimeter as its response has been shown to be independent of therapeutic range beam energies, dose rates, and radiation type (electrons and photons) (Olding *et al* 2010). Electron beams are used for calibration (Babic *et al* 2009) instead of photon beams as the rapid drop-off in the electron depth dose allows us to perform the calibration using a wide range of dose values (from a given dose at D_{max} down to the bremsstrahlung tail), whereas a photon beam depth dose drops-off more slowly ($\sim 50\%$ at the base of a 13 cm tall 1L jar irradiated using 6 MV) producing a smaller range of dose values from which to calibrate the gel. While this calibration technique is commonly referred to as the percent depth dose (PDD) method, it should be noted that our gel dosimetry calibration uses Task Group 51 (Almond *et al* 1999) calibrated clinical electron beams for absolute dosimeter calibration. Calibration gels are irradiated to a given maximum dose which is similar to the maximum dose planned for the measured gel jar.

2.1.4. Gel post-irradiation optical CT scan and reconstruction

After each of the *Measured* and *Calibration* gels have been irradiated, we wait 30 mins in order to allow for the effects of dose development in the Fricke gel to stabilize (Olding and Schreiner 2011). Gels are then imaged using the Vista Optical CT scanner to acquire data (post-irradiation) scans (another 410 projection images). A Feldkamp filtered back projection cone-beam image reconstruction is performed (using commercial software associated with the Vista scanner) and the 3D volume of optical attenuation measurements is then saved as a VFF type file (an image raster file structure originally developed by Sun Microsystems). For the data presented in this paper, all gel imaging is reconstructed to 0.5 mm cubic voxel resolution, unless stated otherwise.

2.2. Overview of the Gel Dosimetry Analysis slicelet

Once the gel dosimeter volumes have been reconstructed and the treatment planning DICOM files are exported from Eclipse, the 3D Slicer Gel Dosimetry Analysis slicelet can be used. The slicelet has four primary components (shown pictorially in figure 3): Data Import, Registration, Calibration, and Dose Comparison. Each component of the slicelet will be detailed in the following sections. 3D Slicer version 4.9 was used in this paper.

2.2.1. Data import

In the slicelet, DICOM files (a series of planning CT images and CBCT images, radiation dose, and structures) and reconstructed 3D optical CT data files (VFF type) for both the measured and calibration gels are imported. In this first step of the slicelet, each loaded volume is assigned its appropriate role. While literature widely describes the use of DICOM files in SlicerRT (Pinter *et al* 2012, Burleson *et al* 2015, Pinter *et al* 2015, Poulin *et al* 2017), the use of VFF files is less common. In the current work we have used VFF and DICOM files (which are both currently acceptable input formats), however the 3D Slicer environment enables the development of custom tools which could allow for other file types to be imported, incorporated into the workflow, and visualized in 3D Slicer.

2.2.2. Registration

The treatment planned dose volume and the irradiated gel volume must be registered in order to compare the two and draw conclusions about the accuracy of the dose delivery. This is achieved by registering all volumes (planning data and optical CT gel data) to the common CBCT volume space, as shown in figure 4. Historically, registration was performed using CERR and custom Matlab scripts which enabled manual alignment of two datasets and allowed for fiducial registration by using a 4–6 point translate-rotate rigid body registration. Using this former method, both the reference and measured data were interpolated to a common grid, introducing the possibility of additional interpolation related uncertainties.

The registration is performed in two steps in the slicelet: registering the planning data to the CBCT volume space, and registering the optical CT data (the *Measured* volume) to the CBCT volume space. Each step can be performed using either fiducial registration or automatic image based registration techniques. While registering the planning data (dose volume, structures, and planning CT volume) to the CBCT volume space can be easily performed using either registration technique, the optical CT data and the CBCT volume (Step 2.2 in figure 4) are less likely to register properly due to the symmetry about the central axis of the gel in its cylindrical jar when in the optical CT volume. For this reason, in our work we use fiducial based registration to align the optical CT and CBCT in the same coordinate axes.

2.2.3. Calibration

The gel slicelet calibration process is tailored to the depth dose method, based on using a well characterized standard irradiation with an electron beam and correlating the electron depth dose data from ionization chamber measurements (taken at time of treatment machine commissioning), and comparing it with measured optical attenuation measurements from a gel dosimeter. Since our Fricke gel dosimeter response is linear with increasing dose (Babic

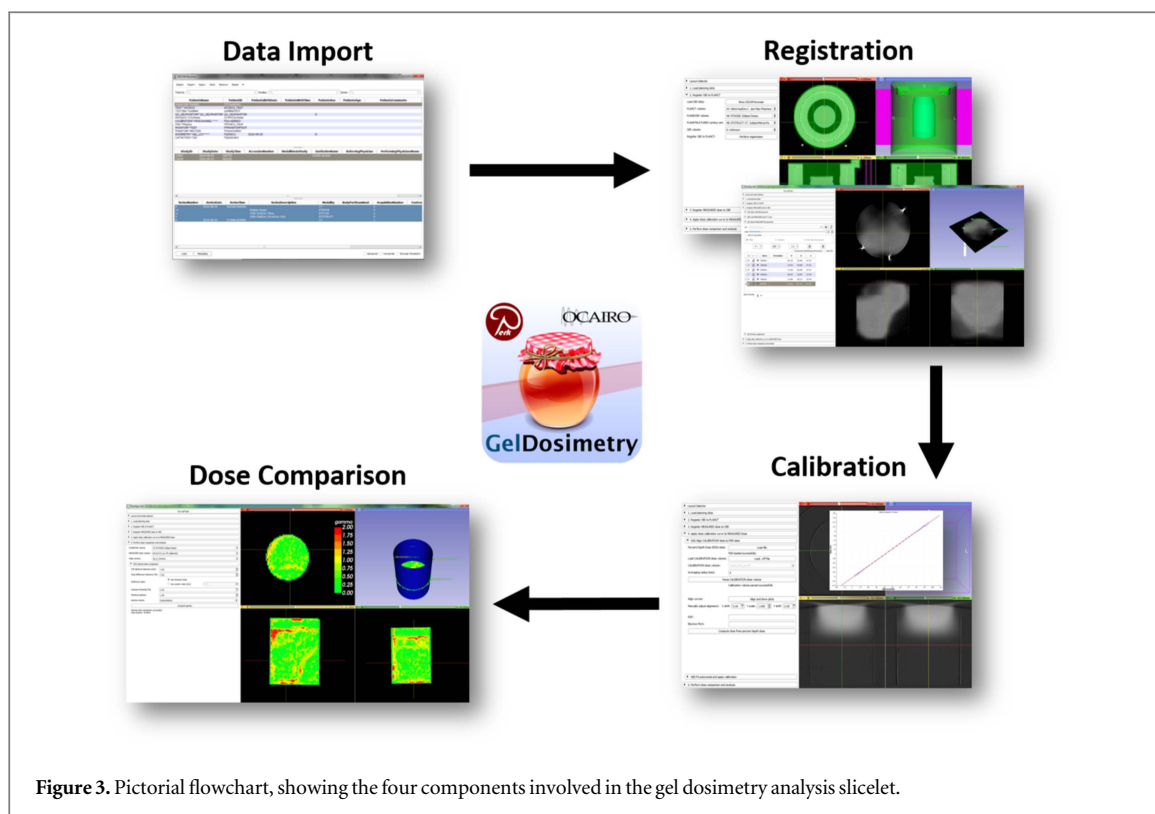


Figure 3. Pictorial flowchart, showing the four components involved in the gel dosimetry analysis slicelet.

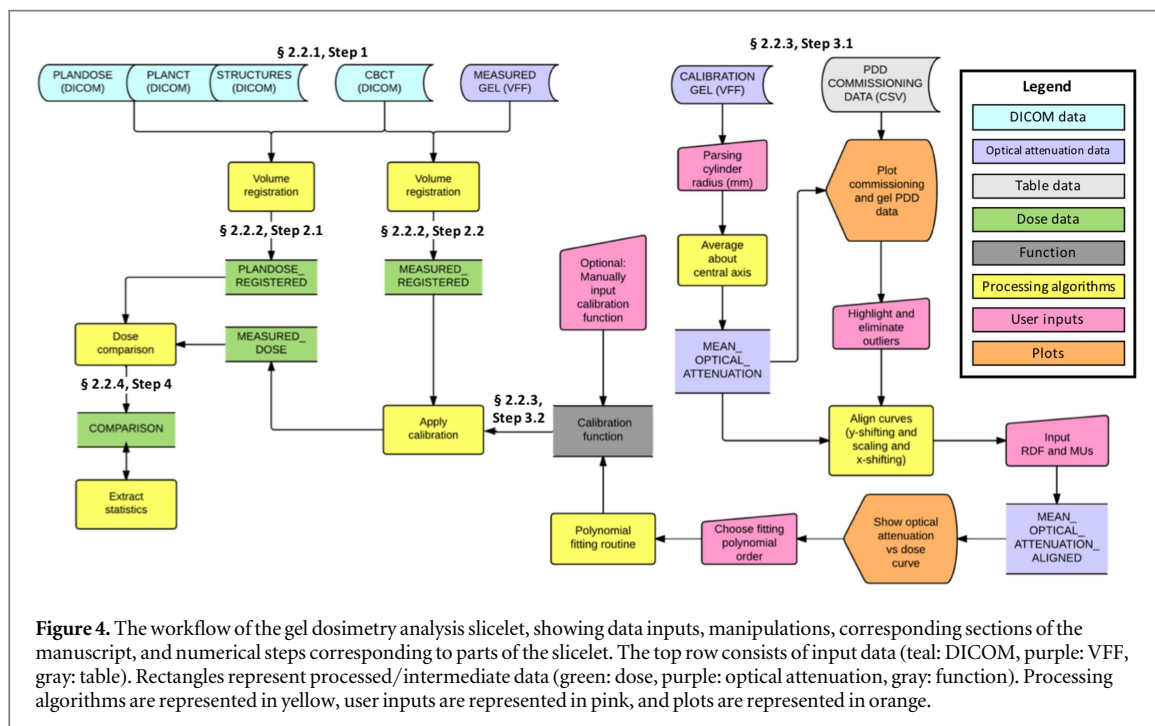
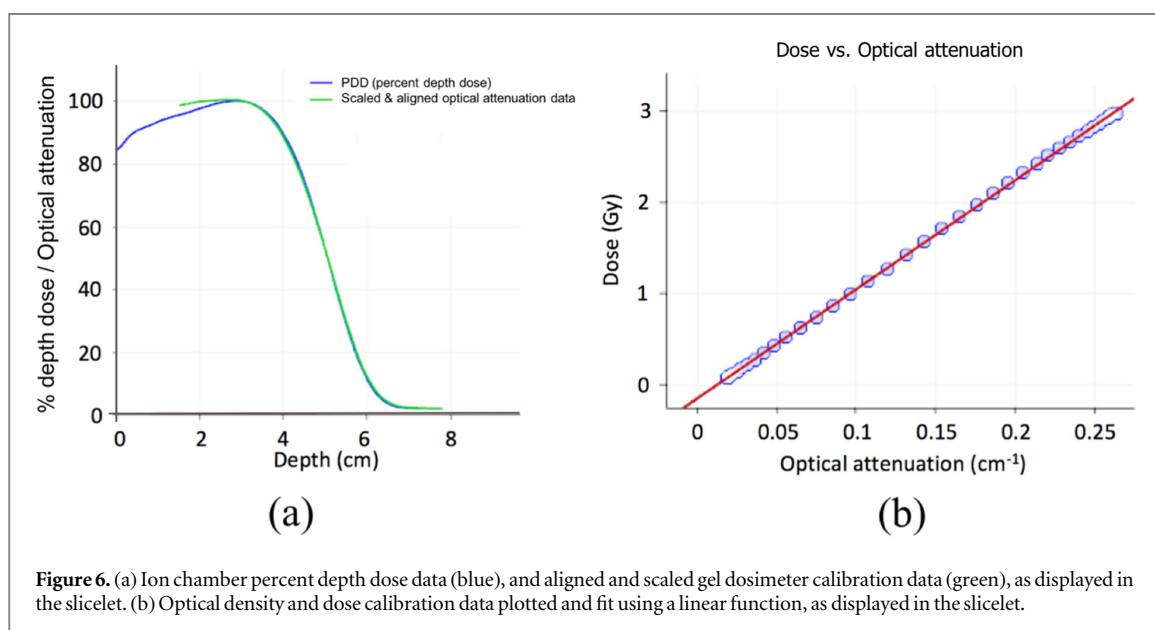
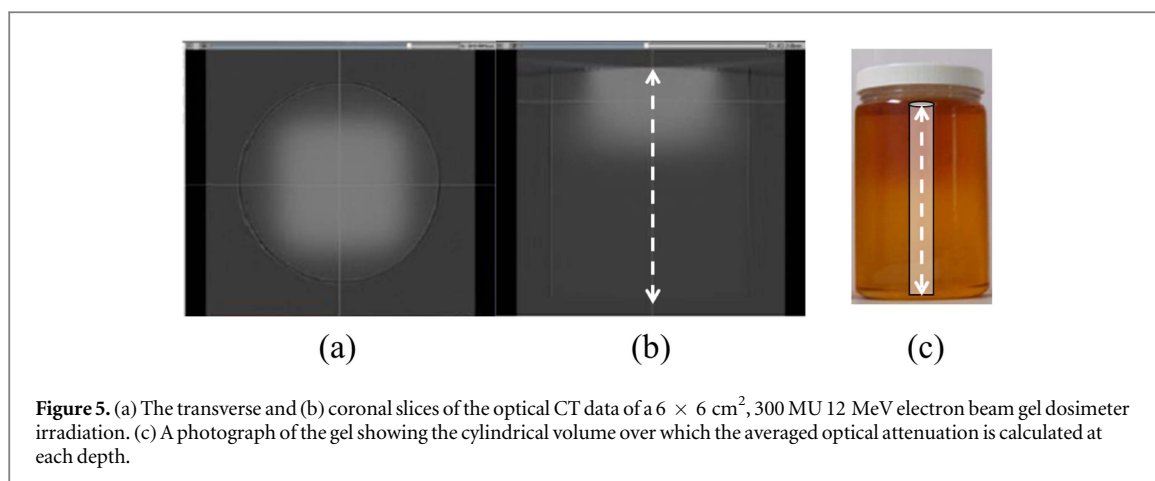


Figure 4. The workflow of the gel dosimetry analysis slicelet, showing data inputs, manipulations, corresponding sections of the manuscript, and numerical steps corresponding to parts of the slicelet. The top row consists of input data (teal: DICOM, purple: VFF, gray: table). Rectangles represent processed/intermediate data (green: dose, purple: optical attenuation, gray: function). Processing algorithms are represented in yellow, user inputs are represented in pink, and plots are represented in orange.

et al 2009), this allows for easy alignment of the two depth dose curves. Historically, the calibration gel optical CT data was imported into Matlab and a profile about the central axis was extracted. This optical attenuation profile was then manually aligned to the commissioning depth dose profile in Microsoft Excel. Corresponding optical attenuation and dose data points were then used to generate a calibration curve.

In this step of the slicelet, a CSV file is imported, which contains the standard electron beam's percent

depth dose data (first column is PDD, and the second column is the depth in centimetres) taken at time of commissioning. The software requires that the relative dose factor (RDF) for the calibration irradiation field and the number of monitor units (MUs) used in the calibration be input accordingly. To improve the signal-to-noise ratio of calibration data points, an average optical attenuation value at each depth is calculated by averaging over a circular disk of radius 5 mm at each depth (figure 5). The commissioning



depth dose and the average optical attenuation depth curves are then plotted on the same axes, and the curves are aligned (figure 6(a)) using the Amoeba optimizer function (Schroeder *et al* 2006), which explores the parameter space of the 2D registration (Y-scaling, Y-shifting, and X-shifting), converging to a minimum of the distance between the two curves. The Y-scaling and Y-shifting in this case are purely cosmetic, as they allow the depth dose data and the optical attenuation depth values to be plotted in the same range. The X-shift is the common parameter over which the optical attenuation depth and depth dose data are aligned. Minor manual adjustments are generally made to each degree of freedom to improve the alignment of the two curves.

From the aligned curves, corresponding optical attenuation and dose points are plotted. Outliers in the optical attenuation data curve, due to reconstruction artefacts caused by internal reflections at the boundary between gel and air at the top of the jar (Jordan and Avvakumov 2009), are removed from the plot. Calibration data is generally taken from the primary calibration reference depth (e.g., 2.9 cm for a 12 MeV

electron beam, SSD = 100 cm) down to the bremsstrahlung tail and is fit to determine a calibration function relating optical attenuation to dose (figure 6). While we use a linear fit, the slicelet also allows for fitting with higher order polynomials if necessary. Calibration data points can also be exported to a spreadsheet CSV file for other purposes.

2.2.4. Dose comparison

Comparing large calculated dose distributions and 3D dose measurements can be difficult. In radiation dosimetry, the gamma comparison tool (Ju *et al* 2008, Low 2010) is commonly used to compare 3D dose datasets, enabling quantitative analysis of agreement between two dose distributions by combining dose-difference and distance-to-agreement criteria.

The final step in the slicelet consists of performing a gamma dose comparison between the treatment planning system dose distribution and the measured gel dose distribution. The dose distributions are automatically assigned with the treatment planning dose distribution as the reference volume and the calibrated gel distribution as the evaluated volume (figure 7). The

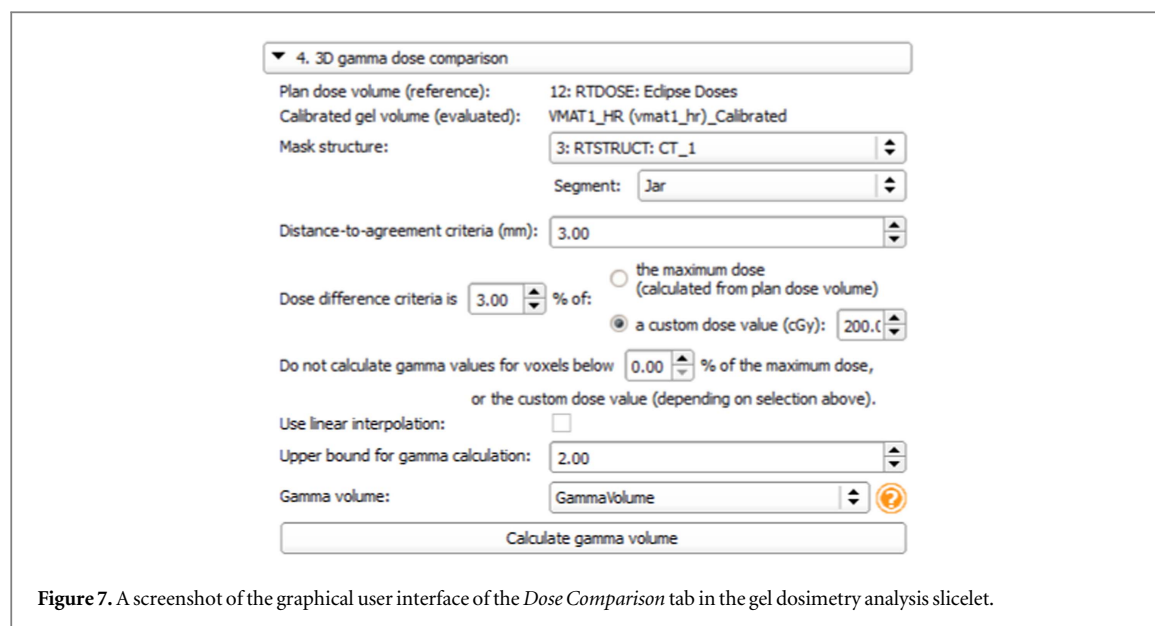


Figure 7. A screenshot of the graphical user interface of the *Dose Comparison* tab in the gel dosimetry analysis slicelet.

distance-to-agreement is also assigned, and the dose difference criteria is set as either a percentage of the maximum dose in the planned dose volume or a percentage of a custom, user defined dose value (i.e., prescription dose). A particular structure can be selected in which to calculate gamma values, a low dose threshold can be set, and options to use linear interpolation and set an upper bound on the gamma calculation can be selected.

After a gamma dose comparison has been performed, each voxel in the evaluated dose distribution is said to be in agreement with the reference dose volume under the assigned Δd and ΔD tolerances when $\gamma \leq 1$. The gamma pass rate is defined as the fraction of voxels in some volume of interest, where $\gamma \leq 1$.

The general implementation of the gamma comparison in SlicerRT allows for the gamma comparison to be performed across any volume. However, when using the gel slicelet, our practice is to choose the contoured gel dosimeter jar structure. Using the upper bound option also restricts the search region for efficiency (i.e., upper bound of 2 translates into a maximum search region of under 4.5 mm). Calculating and displaying the entire gamma volume is an attractive feature of the slicelet, as a full 3D gamma calculation is more clinically relevant than just reporting a pass rate, which can easily mask delivery problems.

2.3. Slicelet validation experiments

Numerous experiments through various test configurations have been used to evaluate the four steps (shown pictorially in figure 3 and as a detailed workflow in figure 4). The design of the slicelet is reviewed here to ensure that it is reliable and accurate.

Table 1. Descriptions of gamma dose comparison test datasets.

Dataset 1	Reference volume:	Four field box, simulated using Eclipse (1 mm resolution)
	Evaluated volume:	Modified four field box (1 mm resolution) Field 1: Spatial shift (3 mm) Field 2: 8% increase in monitor units Field 3: 45° dynamic wedge Field 4: No change
Dataset 2	Reference volume:	VMAT plan calculated using Eclipse (2 mm resolution)
	Evaluated volume:	Dose calculated from optical CT gel dosimeter measurement (0.5 mm resolution)

2.3.1. Data import

To ensure that SlicerRT was accurately reading the VFF files, sample VFF files of irradiated gels were imported into Matlab both through SlicerRT, via MatlabBridge (Pinter *et al* 2015) (which enables Matlab functions to be run from within 3D Slicer), and directly (through an in-house script). The two volumes imported by these different means were then compared.

2.3.2. Registration

As described earlier, fiducial dots were inscribed with a marker on the gel jar (visible by optical CT), and then were covered with radio-opaque metal BBs (visible by x-ray CT). In order to check the robustness of the fiducial based registration, the optical CT to CBCT registration step was performed by three different users for two unique gel datasets (each dataset had 6

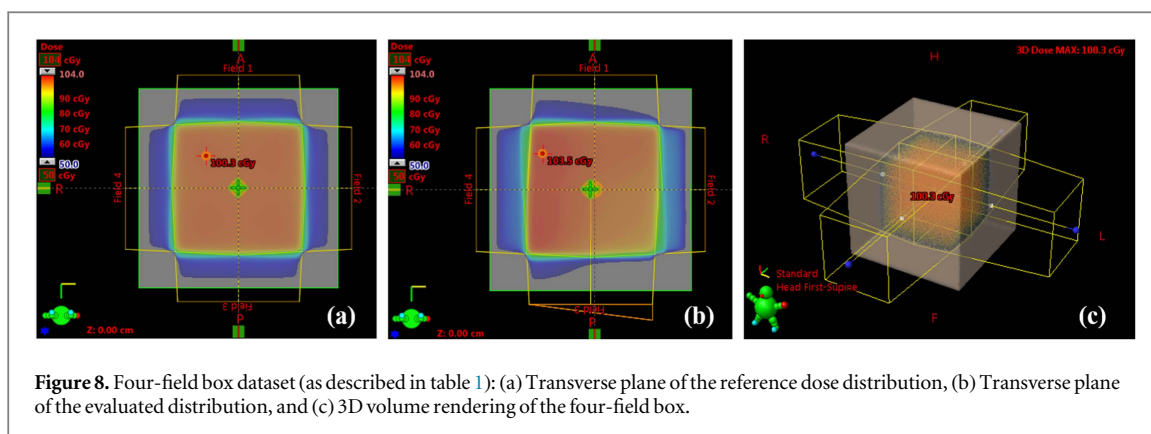


Figure 8. Four-field box dataset (as described in table 1): (a) Transverse plane of the reference dose distribution, (b) Transverse plane of the evaluated distribution, and (c) 3D volume rendering of the four-field box.

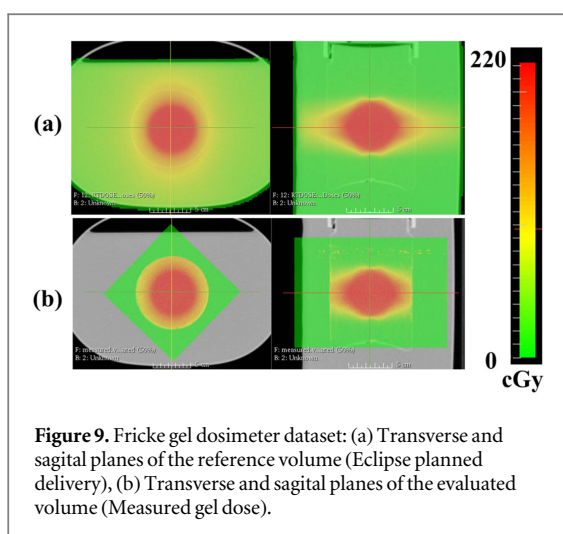


Figure 9. Fricke gel dosimeter dataset: (a) Transverse and sagittal planes of the reference volume (Eclipse planned delivery), (b) Transverse and sagittal planes of the evaluated volume (Measured gel dose).

fiducial points). The root mean square error (RMSE) was calculated for each user and dataset.

Since the accuracy of the automatic image based registration technique can vary depending on the specific dataset due to symmetrical features and image noise, this component of the slicelet was validated using three unique irradiations on three unique phantoms (each study consisted of a dose volume, planning CT, and CBCT from a gel dataset). One dataset used a small gel jar (~400 ml total volume) and two datasets featured larger jars (~1 L total volume). The automatic image-based registration has many parameters. The sole registration parameter that was modified (when compared to the default SlicerRT settings) emphasized translational motion over rotational motion in the registration. For each dataset, the gel jar had previously been contoured (cylindrical volume, starting at the shoulder of the jar and down to the plastic dimple on the bottom of the jar) on the planning CT volume using Eclipse, and the CBCT volume had a gel jar structure manually added by using the Segment Editor module in 3D Slicer. The automatic image registration tool was then used to register the planning CT and structures to the CBCT image space. Depending on the geometry of the imaged phantom, the registration sometimes required several iterations in order to

achieve a visually accurate registration. While not used in the validation of this step, manual translation/rotation adjustments can be made after using the automated image based registration.

The SlicerRT Segment Comparison tool was used to compare the two jar structures once the volumes were registered. This tool calculates both the Hausdorff distance (Huttenlocher *et al* 1993) (measurement of the mismatch of two structures), and dice similarity metrics (Dice 1945) (a coefficient expressing the amount of overlap between the structures). These metrics for each dataset and volumes for each gel jar structure were calculated.

2.3.3. Calibration

In order to validate the calibration step of the software, both the consistency of calibration measurements and inter-user variability of the process were tested. Two batches of Fricke xylene orange gel dosimeter were manufactured and poured into two 1-litre clear jars (total 4 jars). For each irradiation, the jar was centred under the electron beam with the jar lid removed. Jars were irradiated to 300 MU, using three different energies (9, 12, and 16 MeV), with a repetition of the 12 MeV beam irradiation in each gel batch. To determine the consistency of calibration measurements, the four calibration gel jars were each analyzed five times and the dose sensitivities (which describes how the optical attenuation of the gel changes with increasing dose) of each was calculated. Since it is crucial that the software's calibration results are independent of user, the inter-user variability was tested by three different medical physics researchers who independently used the slicelet to determine the dose sensitivity of each gel jar.

2.3.4. Dose comparison

To ensure the accuracy of the gamma comparison module, we cross-validated the SlicerRT algorithm (written by other SlicerRT contributors Sharp *et al* 2010) with our independently developed, in-house algorithm (written in Matlab) using simulated and measured dose distributions. The results from the SlicerRT gamma dose comparison tool were

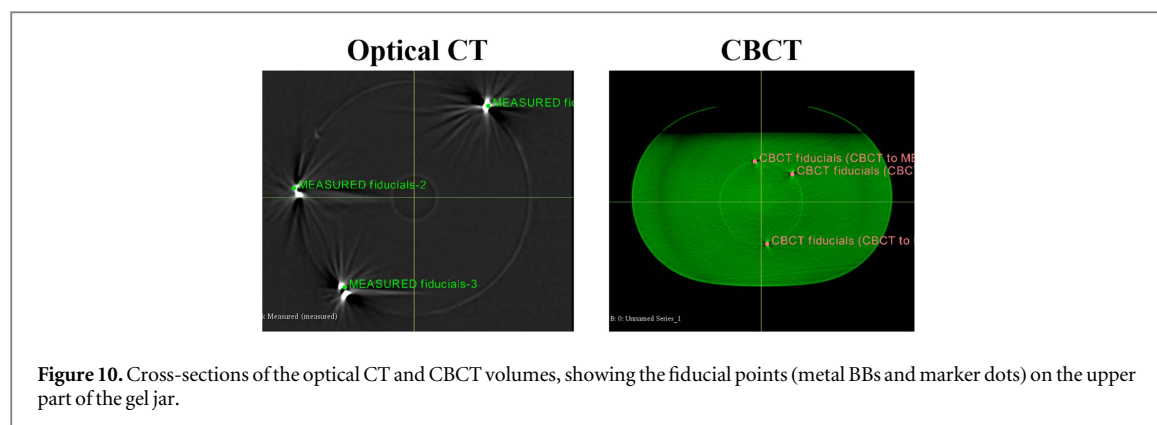


Figure 10. Cross-sections of the optical CT and CBCT volumes, showing the fiducial points (metal BBs and marker dots) on the upper part of the gel jar.

Table 2. RMSE for registration performed in registering the CBCT and optical CT data.

	User 1	User 2	User 3
	RMSE	RMSE	RMSE
	(mm)	(mm)	(mm)
Dataset 1	1.26	0.95	1.23
Dataset 2	0.85	1.02	0.81

Table 3. Dice similarity coefficients, Hausdorff distance metrics, and volumes of the gel jar structure used for comparison for three separate datasets.

	Dataset #1	Dataset #2	Dataset #3
Dice similarity coefficient	0.98	0.99	0.98
Hausdorff distance metrics			
Average (mm)	0.46	0.30	0.83
Maximum (mm)	3.52	1.66	1.84
95% (mm)	1.60	1.17	1.29
Volume of planning CT jar structure (cc)	317.2	819.4	810.2
Volume of CBCT jar structure (cc)	324.4	814.7	808.5

Table 4. Mean sensitivities for electron beam gel dosimeter irradiations (Alexander *et al* 2015).

Gel batch	Electron beam energy (MeV)	Mean sensitivity ($\text{cm}^{-1} \text{Gy}^{-1}$) \pm Relative std. dev.
A	9	$0.0840 \pm 0.1\%$
A	12	$0.0830 \pm 0.1\%$
B	12	$0.0849 \pm 0.1\%$
B	16	$0.0872 \pm 0.1\%$

compared to results from our in-house gamma algorithm by using MatlabBridge (Pinter *et al* 2015) (an extension in 3D Slicer) which enabled the calculated SlicerRT gamma volume to be exported to Matlab for comparison with our in-house algorithm. Both point-to-point and interpolation-based (Ju *et al* 2008) gamma algorithms were tested.

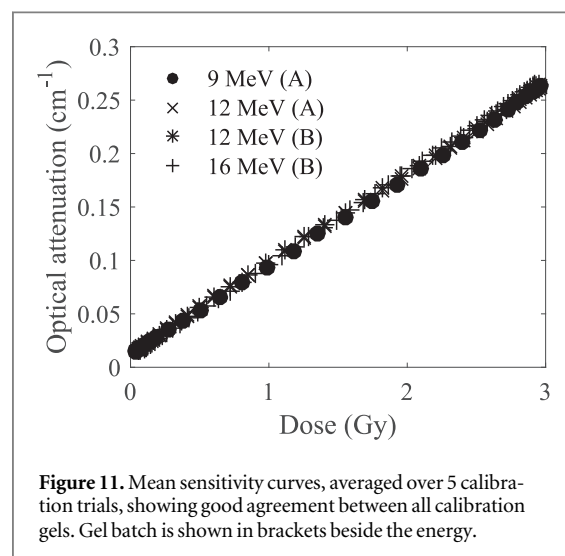


Figure 11. Mean sensitivity curves, averaged over 5 calibration trials, showing good agreement between all calibration gels. Gel batch is shown in brackets beside the energy.

Two 3D dose datasets were used for cross-validation of the algorithms, as described in table 1 and shown in figures 8 and 9. The first dataset consisted of a simulated four-field box irradiation delivered to a plastic water phantom as the reference dose volume (prescription dose of 100 cGy at the isocenter). Inspired by the 2D example detailed in Low and Dempsey (2003), the reference distribution was then modified within Eclipse to create an evaluated dose distribution by spatially shifting one field by 3 mm, increasing the monitor units of the second field by 8%, applying a dynamic wedge for the third field, and leaving the fourth field unchanged to produce the evaluated dose volume. The second dataset consisted of a VMAT plan delivered to a gel dosimeter phantom. The reference dose volume was a calculated VMAT Eclipse treatment plan delivered to a jar of Fricke gel in a water tank, and the evaluated dose volume was calculated from optical CT measurements of the Fricke gel.

In this work, a 3%/3 mm gamma criteria was used unless otherwise stated. The dose difference criteria in the slicelet was explicitly defined by setting the dose difference criteria to be 3% of the reference prescription dose, which was input for each dataset (see figure 7). No low dose threshold was required or used. For dataset 2, the data within 5 mm of the gel jars walls

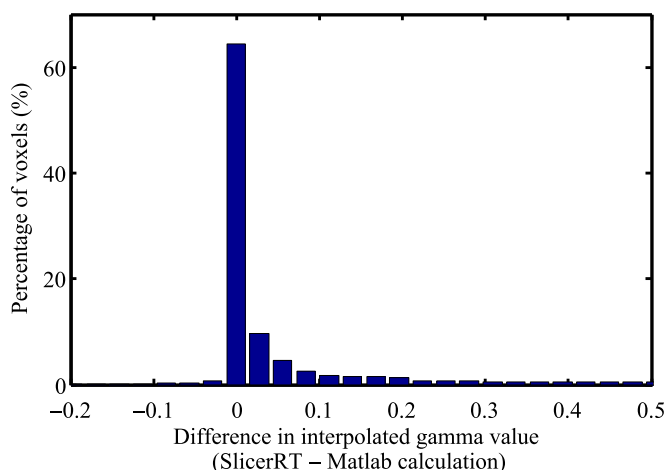


Figure 12. 85% of gamma voxels were found to vary by less than ± 0.1 when results from interpolation-based SlicerRT and interpolation-based Matlab gamma algorithms were compared.

Table 5. Inter-user variation of gel sensitivities for three different users. Individual user determined sensitivities, mean sensitivities, and relative standard deviations are presented for each gel (Alexander *et al* 2015).

Electron beam energy (MeV)	User 1 ($\text{cm}^{-1} \text{Gy}^{-1}$)	User 2 ($\text{cm}^{-1} \text{Gy}^{-1}$)	User 3 ($\text{cm}^{-1} \text{Gy}^{-1}$)	Mean sensitivity ($\text{cm}^{-1} \text{Gy}^{-1}$) \pm Relative std. dev.
9	0.0839	0.0841	0.0841	$0.0840 \pm 0.1\%$
12	0.0828	0.0836	0.0829	$0.0831 \pm 0.5\%$
12	0.0841	0.0837	0.0847	$0.0842 \pm 0.6\%$
16	0.0871	0.0870	0.0872	$0.0871 \pm 0.1\%$

Table 6. Point-to-point gamma algorithm pass rates (3%, 3 mm) for two test cases for a range of resolutions. At finer resolutions, the evaluated distribution approaches a continuous distribution, giving a gamma distribution approaching the theoretical minimum.

Resolution	Four field box pass rate	Gel dosimeter pass rate
0.5 mm	89.9%	97.1%
1 mm	88.4%	96.0%
2 mm	86.4%	90.0%
3 mm	81.2%	47.4%

Table 7. Point-to-point algorithm gamma pass rates (3%, 3 mm) for the gel dosimeter case, with the roles of reference and evaluated distributions exchanged. Noisy gel dosimeter measurements yield a more forgiving comparison in the role of evaluated distribution by providing a range of dose values in close proximity to each reference point.

	Gel dosimeter pass rate
Reference: Calculated dose Evaluated: Measured gel dose	96.0%
Reference: Measured gel dose Evaluated: Calculated dose	91.1%

was not used in the evaluation. An upper bound of 2 was used for all gamma calculations, and gamma values were calculated for all space for the simulated four-field box dataset, and within the gel jar for the second dataset. For both datasets, different resolutions were tested using a point-to-point gamma comparison, as was the effect of exchanging the roles of the reference and evaluated distributions. For the gamma analysis, the 3D datasets were registered but not interpolated. For dataset 2, the lower resolution planning data was the reference distribution and the higher resolution measurement dataset was searched using the gamma evaluation. The gamma evaluation results were reported at the resolution of the reference distribution.

3. Results and discussion

3.1. Data import

As described in section 2.2.1, DICOM files and reconstructed 3D optical CT VFF files can easily be read into 3D Slicer. One of the significant improvements of using 3D Slicer over our previous analysis method, is that 3D Slicer organizes DICOM CT images, dose files, and structures using a DICOM Browser (similar to a patient browser in a treatment planning system). Importing and viewing both DICOM and VFF volumes is simple and switching views and planes of different volumes in 3D Slicer is

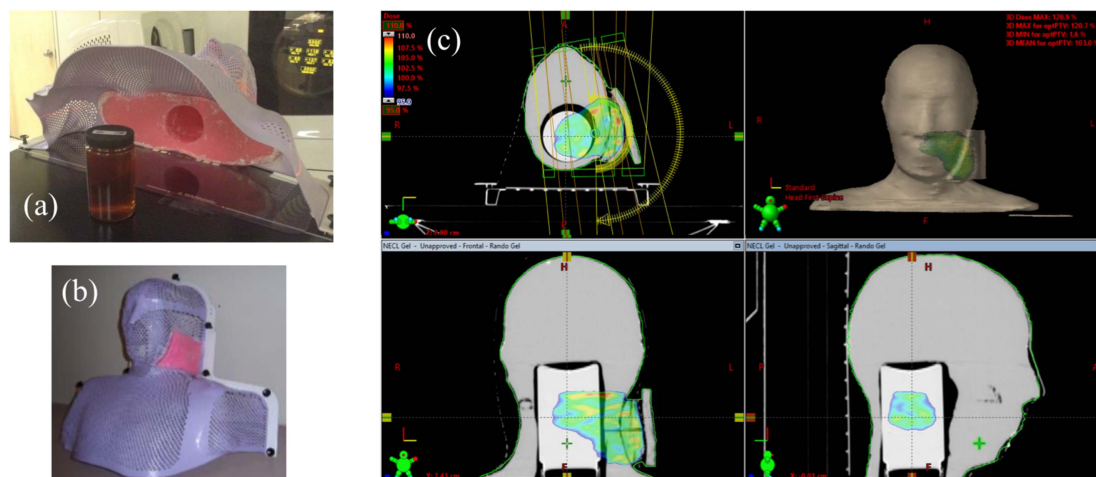


Figure 13. (a) Photo of the Fricke gel dosimeter jar and pink wax head and neck phantom (showing interior neck cavity for the gel jar). (b) Thermoplastic head and neck mask used to immobilize the phantom and build-up wax bolus to enable better dose conformity to the neck. (c) Screenshot of the Eclipse planning system, showing the VMAT plan delivered to the wax phantom with gel jar insert. A Philips Brilliance Big Bore CT scanner (Philips Medical Systems, Cleveland, OH) was used and for planning with 2 mm isotropic resolution. Delivery was via volumetric modulated arc therapy (VMAT) consisting of two 6 MV coplanar partial arcs. The planned dose delivery was calculated using Eclipse v.10 (Varian Medical Systems, Palo Alto, CA). The tumour was prescribed a dose of 1.8 Gy, which was delivered using a Varian Trilogy 2100iX linear accelerator (Varian Medical Systems, Palo Alto, CA), which features OBI cone beam CT (CBCT) imaging capability to verify patient alignment. Automatic image based registration was used as in step 2.1 of the slicelet. In step 2.2, three coplanar fiducial points (BBs and underlying pen markings) at the top of the jar were chosen on each of the optical CT volume and the CBCT volume. The optical CT volume was then registered to the CBCT volume with a RMSE of 0.97 mm.

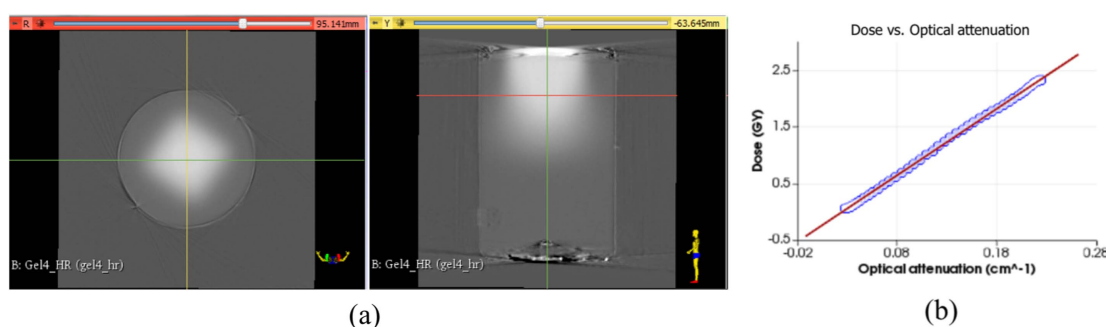


Figure 14. (a) Screenshot showing slices through the optical CT data of a 3×3 cm², 250 MU 12 MeV electron beam Fricke gel dosimeter irradiation. (b) Optical attenuation and dose calibration data points and a linear fit line.

quick. This was not possible using the previous analysis method.

A comparison of a VFF file imported into Matlab, and the same file imported into SlicerRT and then exported to Matlab showed no difference between the two volumes, meaning that both file importers are identical.

3.2. Registration

The RMSE for two different gel datasets (registering an optical CT volume to a CBCT volume) was calculated for the registrations as performed by three different users. Users selected six unique fiducial points in each volume (three at the top of the jar, and three towards the bottom of the jar), as indicated by the highly

attenuating marker dots on the optical CT and the metal BBs on the CBCT (figure 10). The RMSE for each set of corresponding points was calculated, as shown in table 2, and showed submillimeter variation in the registration process between users.

Once the dataset volumes were registered using the automatic image based registration, the physical volume of the contoured gel jars, Hausdorff distances, and dice similarity metrics were calculated by comparing the jar structure on the planning CT volume to the jar structure on the CBCT volume (table 3). The physical volumes of the gel jars for each dataset were calculated using the jar structures and show good consistency between the two imaging volumes. Average Hausdorff distances for all three datasets examined

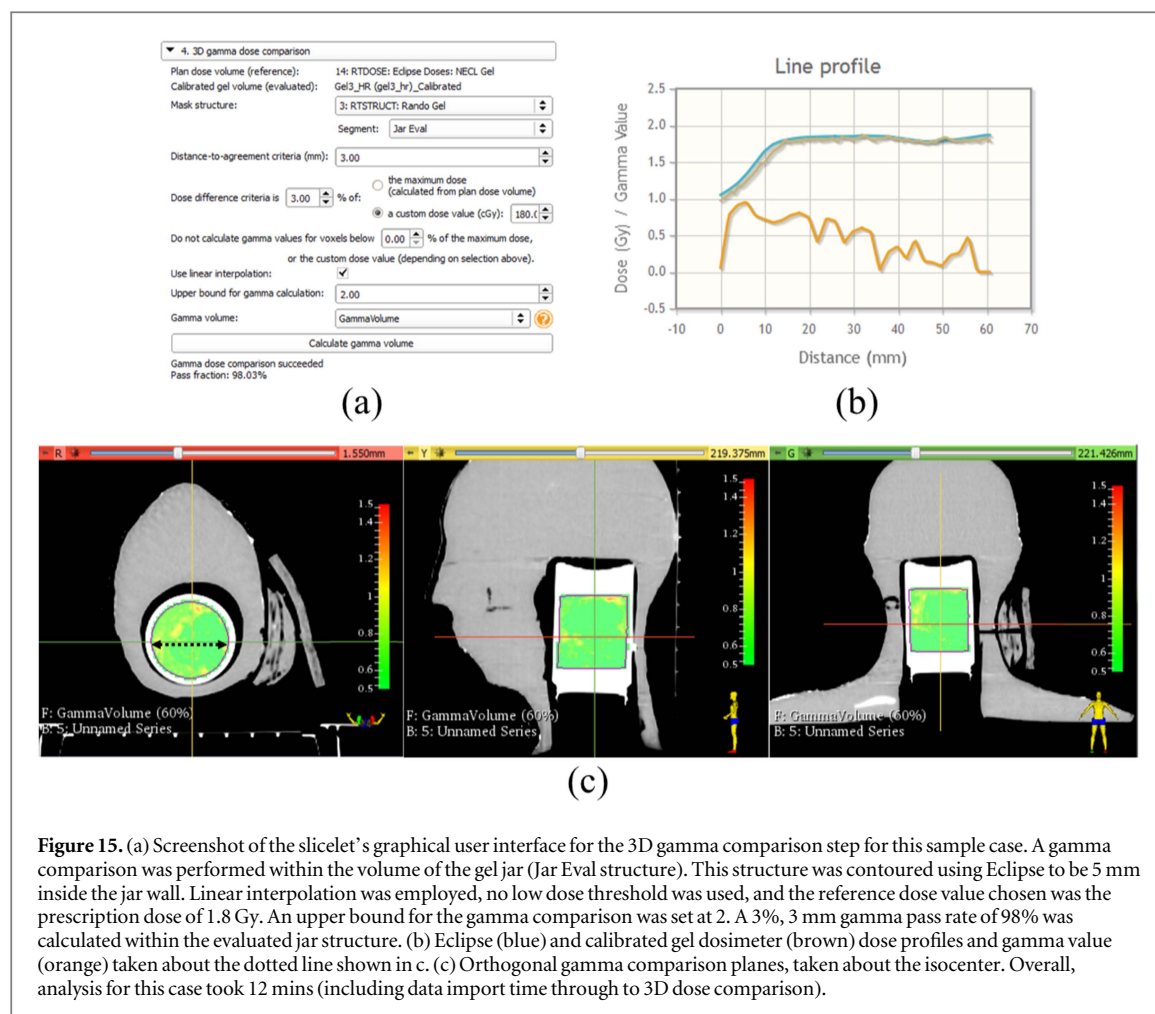


Figure 15. (a) Screenshot of the slicelet's graphical user interface for the 3D gamma comparison step for this sample case. A gamma comparison was performed within the volume of the gel jar (Jar Eval structure). This structure was contoured using Eclipse to be 5 mm inside the jar wall. Linear interpolation was employed, no low dose threshold was used, and the reference dose value chosen was the prescription dose of 1.8 Gy. An upper bound for the gamma comparison was set at 2. A 3%, 3 mm gamma pass rate of 98% was calculated within the evaluated jar structure. (b) Eclipse (blue) and calibrated gel dosimeter (brown) dose profiles and gamma value (orange) taken about the dotted line shown in c. (c) Orthogonal gamma comparison planes, taken about the isocenter. Overall, analysis for this case took 12 mins (including data import time through to 3D dose comparison).

were under 1 mm, and the 95% Hausdorff distance shows that 95% of the jar volumes were aligned to within 1.60 mm of each other. Dice similarity coefficients were also very high, indicating good agreement between the registered volumes. These results show that the automatic image based registration is robust and aligns the planning data to the CBCT volume quite well. While not used in this validation work, slight manual translations/rotations of the planning CT volume can be performed after automated registration (if the automated registration produces obviously misaligned imaging volumes) which may improve these metrics. Overall, these registration tools are a significant improvement over the previously used and tedious manipulations performed in Matlab/CERR.

3.3. Calibration

The dose calibration procedure in step 3 of the slicelet was performed five times, for four different gel jars. Dose sensitivity curves (inverse of the calibration plot in figure 6(b)) were consistent over five trials with a relative standard deviation of 0.1% (table 4, figure 11). Overall, a mean dose sensitivity of $0.084 \text{ cm}^{-1} \text{ Gy}^{-1}$ (relative standard deviation of 2%) was determined across all irradiated gels at the different electron beam energies.

In the inter-user variability study, the mean dose sensitivity for the all gel jars was found to have relative standard deviations up to 0.6% across three users (table 5). These dose sensitivities also agreed with the findings in table 5, and show that results are consistent and that various users were able to replicate the gel calibration process and achieve similar dose sensitivities.

The calibration process has been streamlined by the slicelet and makes the calibration procedure more robust and less prone to human errors when manipulating data. While we use an absolute depth dose calibration method in our clinic, other calibration methods could easily be added as options to the slicelet, or calibration functions can be determined external to the slicelet and then be manually input.

3.4. Dose comparison

Excellent agreement was found between the gamma results obtained using the point-to-point SlicerRT dose comparison tool and our in-house point-to-point gamma algorithm implemented in Matlab for both the four-field box and gel datasets. The implementation of the gamma comparison algorithm in SlicerRT is substantially faster as a full 3D comparison is complete in under one minute, whereas the gamma comparison algorithm in Matlab would take up to one hour, depending on the size of calculation volume.

When comparing results from interpolation-based SlicerRT and interpolation-based Matlab gamma algorithms, 85% of gamma voxels were found to vary by less than ± 0.1 (figure 12). This result was anticipated as the choice of interpolation parameters (i.e., sample step size) heavily influences gamma results (Wendling *et al* 2007). The behaviour of the SlicerRT gamma dose comparison algorithm with respect to resolution and the role of the reference and evaluated dose distributions was found to be consistent with previous findings (tables 6 and 7).

For further comparisons, a dose line profile tool can be used to plot profiles that compare the calibrated gel measurement and the calculated dose distribution. Gamma values can also be plotted along the same profile.

4. Conclusion

The development of a fast, convenient, and robust 3D dose analysis environment for gel dosimetry presents a significant step in making gel dosimetry more accessible. When compared to our previous analysis process, the slicelet has made gel analysis roughly 20 times faster, with a typical analysis of the 3D dose in a 1L volume complete within 15 min. We have shown that imaging data is correctly imported, and that registration techniques are robust and register volumes with millimeter precision. Gel dosimeter calibration was proven to be precise and highly reproducible across several different users, and the point-to-point gamma dose comparison was shown to match our pre-existing Matlab gamma code.

In recent years, we have presented several international workshops which have helped users learn about this new analysis tool. Tutorials have also been made publicly available. Those who are interested in using the slicelet should download and install 3D Slicer from <http://slicer.org>, and then install the SlicerRT and Gel Dosimetry Analysis extensions from within 3D Slicer. More information and tutorials can be found at <http://slicer.org/wiki/Documentation/Nightly/Modules/GelDosimetry>.

Moving forward, there is potential to create other versions of the slicelet that cater to different gel dosimeter readout modalities, such as magnetic resonance, or for other 2D/3D dosimetry systems. Overall, this open-source and free software in 3D Slicer removes one more hurdle for those interested in using gel dosimeters.

Acknowledgments

This work was funded by the Canadian Institutes for Health Research (CIHR), funding project MOP-115101. The authors wish to acknowledge the contributions of Chris Jechel, Mattea Welch, Jennifer Andrea, and several beta users who helped identify needed improvements.

Appendix—sample gel study using the gel dosimetry analysis slicelet

To illustrate a typical workflow using the Gel Dosimetry Analysis slicelet, we present a radiation therapy treatment delivered to an anthropomorphic head and neck phantom. This phantom was used in Alexander *et al* (2017) and consists of a wax head and neck phantom (which was created by pouring wax into a plaster mould of a Rando phantom), designed with a cavity in the neck to fit a gel dosimeter jar (figure 13). A removable neck tumour (thickest part measuring 2.6 cm) was designed to fit just below the ear of the phantom. The phantom was immobilized using a thermoplastic mask during CT planning and radiation treatment plan delivery, and wax build-up was placed on top of the mask over the tumour region. While the phantom was built in-house and air gaps are present between the different layers of wax (namely in the neck tumour, see figure 13), this is not a problem since the radiation treatment plan was calculated on the CT data of the phantom with its inserts and air gaps. Calibration and dose comparison for this sample gel study is shown in figures 14 and 15, respectively.

ORCID iDs

K M Alexander  <https://orcid.org/0000-0001-7398-4264>

C Pinter  <https://orcid.org/0000-0001-9982-3194>

References

- Adamovics J and Maryanski M J 2006 Characterisation of PRESAGE: a new 3-D radiochromic solid polymer dosimeter for ionising radiation *Radiat. Prot. Dosim.* **120** 107–12
- Alexander K M, Gooding J, Schreiner L J and Olding T 2017 Clinical management of tumour volume changes in VMAT head & neck radiation treatment *Journal of Physics: Conference Series* **847** 012038
- Alexander K M, Pinter C, Andrea J, Fichtinger G and Schreiner L J 2015 3D slicer gel dosimetry analysis: validation of the calibration process World Congress on Medical Physics and Biomedical Engineering, June 7–12, 2015, Toronto, Canada (*IFMBE Proceedings* 51) ed D A Jaffray (Switzerland: Springer International Publishing) (https://doi.org/10.1007/978-3-319-19387-8_128)
- Almond P R, Biggs P J and Hanson W F 1999 AAPM's TG-51 protocol for clinical reference dosimetry of high-energy photon and electron beams *Med. Phys.* **26** 1–9
- Arjomandy B, Sahoo N, Ding X and Gillin M 2008 Use of a two-dimensional ionization chamber array for proton therapy beam quality assurance *Med. Phys.* **35** 3889
- Ascención Y, Dietrich J, Mequanint K and Penev K I 2017 Tetrazolium salt monomers for gel dosimetry II: dosimetric characterization of the ClearView 3D dosimeter *Journal of Physics: Conference Series* **847** 012049
- Babic S, Battista J and Jordan K 2008 An apparent threshold dose response in ferrous xylenol-orange gel dosimeters when scanned with a yellow light source *Phys. Med. Biol.* **53** 1637–50
- Babic S, Battista J and Jordan K 2009 Radiochromic leuco dye micelle hydrogels: II. Low diffusion rate leuco crystal violet gel *Phys. Med. Biol.* **54** 6791–808

- Babic S, McNiven A, Battista J and Jordan K 2009 Three-dimensional dosimetry of small megavoltage radiation fields using radiochromic gels and optical CT scanning *Phys. Med. Biol.* **54** 2463–81
- Burleson S, Baker J, Hsia A T and Xu Z 2015 Use of 3D printers to create a patient-specific 3D bolus for external beam therapy *Journal of Applied Clinical Medical Physics* **16** 166–78
- Devic S 2011 Radiochromic film dosimetry: past, present, and future *Phys. Medica* **27** 122–34
- Dice L R 1945 Measures of the amount of ecologic association between species *Ecology* **26** 297–302
- Guo P Y, Adamovics J A and Oldham M 2006 Characterization of a new radiochromic three-dimensional dosimeter *Med. Phys.* **33** 1338–45
- Huttenlocher D P, Klanderman G A and Rucklidge W J 1993 Comparing images using the Hausdorff distance *IEEE Trans. Pattern Anal. Mach. Intell.* **15** 850–63
- Jordan K and Avvakumov N 2009 Radiochromic leuco dye micelle hydrogels: I. Initial investigation. *Phys. Med. Biol.* **54** 6773–89
- Ju T, Simpson T, Deasy J O and Low D A 2008 Geometric interpretation of the γ dose distribution comparison technique: interpolation-free calculation *Med. Phys.* **35** 879
- Kozicki M, Maras P and Karwowski A C 2014 Software for 3D radiotherapy dosimetry validation *Phys. Med. Biol.* **59** 4111–36
- Li J, Yan G and Liu C 2009 Comparison of two commercial detector arrays for IMRT quality assurance *Journal of Applied Clinical Medical Physics* **10** 2–74
- Low D 2010 Gamma dose distribution evaluation tool *Journal of Physics: Conference Series* **250** 012071
- Low D 2015 The importance of 3D dosimetry *Journal of Physics: Conference Series* **573** 012009
- Low D A and Dempsey J F 2003 Evaluation of the gamma dose distribution comparison method *Med. Phys.* **30** 2455
- Menegotti L, Delana A and Martignano A 2008 Radiochromic film dosimetry with flatbed scanners: a fast and accurate method for dose calibration and uniformity correction with single film exposure *Med. Phys.* **35** 3078
- Mijnheer B, Mans A, Olaciregui-Ruiz I, Sonke J J, Tielenburg R, Van Herk M, Vijlbrief R and Stroom J 2010 2D AND 3D dose verification at The Netherlands Cancer Institute-Antoni van Leeuwenhoek Hospital using EPIDs *Journal of Physics: Conference Series* **250** 012020
- Murphy P and Baldock C 2000 Research software for radiotherapy gel dosimetry *Australas Phys. Eng. Sci. Med.* **23** 44–51
- Nasr A T, Alexander K M, Olding T, Schreiner L J and McAuley K B 2015 Leuco-crystal-violet micelle gel dosimeters: II. Recipe optimization and testing *Phys. Med. Biol.* **60** 4685
- Oldham M, McJury M, Baustert I B, Webb S and Leach M O 1998 Improving calibration accuracy in gel dosimetry *Physics in Medicine & Biology* **43** 2709
- Olding T, Alexander K M, Jechel C, Nasr A T and Joshi C 2015 Delivery validation of VMAT stereotactic ablative body radiotherapy at commissioning *Journal of Physics: Conference Series* **573** 012019
- Olding T, Darko J and Schreiner L J 2010 Effective management of FXG gel dosimetry *Journal of Physics: Conference Series* **250** 129–33
- Olding T, Garcia L, Alexander K, Schreiner L J and Joshi C 2013 Stereotactic body radiation therapy delivery validation *Journal of Physics: Conference Series* **444** 012073
- Olding T, Holmes O, Dejean P, McAuley K B, Nkongchu K, Santyr G and Schreiner L J 2011 Small field dose delivery evaluations using cone beam optical computed tomography-based polymer gel dosimetry *Journal of medical physics / Association of Medical Physicists of India* **36** 3–14
- Olding T and Schreiner L J 2011 Cone-beam optical computed tomography for gel dosimetry II: imaging protocols *Phys. Med. Biol.* **56** 1259–79
- Penev K I and Mequanint K 2015 Characterization of a commercially-produced chemically stable Fricke gel dosimeter *Journal of Physics: Conference Series* **573** 012078
- Pinter C, Lasso A, Wang A, Jaffray D and Fichtinger G 2012 SlicerRT: radiation therapy research toolkit for 3D slicer *Med. Phys.* **39** 6332
- Pinter C, Lasso A, Wang A, Sharp G C, Alexander K M, Jaffray D and Fichtinger G 2015 Performing radiation therapy research using the open-source SlicerRT toolkit *World Congress on Medical Physics and Biomedical Engineering, June 7-12, 2015, Toronto, Canada (IFMBE Proceedings 51)* ed D A Jaffray (Switzerland: Springer International Publishing) (https://doi.org/10.1007/978-3-319-19387-8_152)
- Poulin E, Boudam K, Pinter C, Kadoury S, Lasso A, Fichtinger G and Ménard C 2017 Validation of MRI to US registration for focal HDR prostate brachytherapy *Brachytherapy* **16** S56–7
- Schreiner L J 2011 On the quality assurance and verification of modern radiation therapy treatment *J Med Phys* **36** 189–91
- Schreiner L J 2015 True 3D chemical dosimetry (gels, plastics): Development and clinical role *Journal of Physics: Conference Series* **573** 012003
- Schroeder W, Martin K and Lorensen B 2006 *The Visualization Toolkit: An Object-Oriented Approach to 3D Graphics* 4th edn (La Vergne, TN: Ingram)
- Sharp G C, Li R, Wolfgang J, Chen G, Peroni M, Spadea M F, Mori S, Zhang J, Shackelford J and Kandasamy N 2010 Plastimatch: An open source software suite for radiotherapy image processing *Proceedings of the XVIth International Conference on the use of Computers in Radiotherapy (ICCR)* (Netherlands: Amsterdam)
- Wendling M, Zijp J J, McDermott L N, Smit E J, Sonke J, Mijnheer B J and van Herk M 2007 A fast algorithm for gamma evaluation in 3D *Med. Phys.* **34** 1647–54
- Xu Y and Wu C S 2010 Sensitivity calibration procedures in optical-CT scanning of BANG® 3 polymer gel dosimeters *Medical Physics* **37** 861–8
- Zeidan O A, Stephenson S A L, Meeks S L, Wagner T H, Willoughby T R, Kupelian P A and Langen K M 2006 Characterization and use of EBT radiochromic film for IMRT dose verification *Med. Phys.* **33** 4064